minerals

MDPI

Article

Utilization of Flotation Wastewater for Separation of Chalcopyrite and Molybdenite by Selective Surface Passivation

Yuwu Guo, Guohua Gu *, Yisheng Zhang, Qingke Li, Su Liao and Yanhong Wang

School of Minerals Processing and Bioengineering, Central South University, Changsha 410083, China; mining123@126.com (Y.G.); zys666@csu.edu.cn (Y.Z.); liqingke2022@163.com (Q.L.); liaosu123@csu.edu.cn (S.L.); yanhong.wang@csu.edu.cn (Y.W.)

* Correspondence: guguohua@126.com

Abstract: In the flotation separation process of a Cu-Mo-W polymetallic ore, the wastewater from the scheelite cleaning flowsheet contains large numbers of residual flocculants and metal ions, and the separation of chalcopyrite and molybdenite requires a large number of environmentally harmful depressants. Therefore, it is necessary to find new methods to reduce the environmental and cost pressures of wastewater treatment and the use of depressants. In this work, the flotation wastewater from the scheelite cleaning flowsheet for the separation of chalcopyrite and molybdenite by selective surface passivation was investigated for the first time. Flotations of single minerals and artificially mixed minerals with or without immersion pretreatment in the presence and absence of aeration were performed. The results showed that pulp pH had no effect on the flotation of either mineral, and a molybdenite recovery of 93.22% with a chalcopyrite recovery of 10.77% was achieved under the conditions of 10 days of immersion pretreatment with aeration, 350 mg/L of kerosene, and 100 mg/L of MIBC. By combining the electrochemical cyclic voltammetry analysis and characterization by XRD and SEM, the selective surface passivation mechanism of chalcopyrite was discussed, which could be due to the coverage of the insoluble oxidation products, especially jarosite. This work has simultaneously achieved the depressant-free flotation separation of molybdenite and chalcopyrite and the reuse of scheelite flotation wastewater, which is of great significance for environmental protection and cost saving.

Keywords: chalcopyrite; molybdenite; flotation wastewater; surface passivation; flotation separation

Citation: Guo, Y.; Gu, G.; Zhang, Y.; Li, Q.; Liao, S.; Wang, Y. Utilization of Flotation Wastewater for Separation of Chalcopyrite and Molybdenite by Selective Surface Passivation. *Minerals* **2024**, *14*, 388. https://doi.org/10.3390/min14040388

Academic Editor: Andrea Gerson

Received: 27 March 2024
Revised: 4 April 2024
Accepted: 7 April 2024
Published: 8 April 2024

1. Introduction

With the continuous development of industrial production, the exploitation and consumption of resources has increased exponentially, which has a profound impact on the environment [1]. In the process of mining and mineral processing, a large amount of wastewater is produced. For instance, flotation process consumes 5-7 tons of water per 1 ton of raw ore [2]. Flotation wastewater is usually reused in industry after necessary treatment [2–5]. However, some harmful pollutants, chemicals, ions, organics, etc., in the wastewater accumulate with increased recycling, which interfere with the flotation process [6]. The deterioration of wastewater not only affects the stability and selectivity of flotation froth but also changes the chemical properties of the mineral surface, which leads to the difficulty in the selective separation of minerals [4,7,8].

In nature, a considerable part of tungsten ore is accompanied by copper-molybdenum ore, forming a Cu-Mo-W polymetallic ore, and in most cases, they exist in the form of scheelite ($CaWO_4$), chalcopyrite ($CuFeS_2$), and molybdenite (MoS_2), respectively [9–11]. Usually, Cu-Mo bulk flotation concentrate is obtained first, then it is separated into chalcopyrite concentrate and molybdenite concentrate [12], and finally scheelite is recovered from the tailings of Cu-Mo bulk flotation [13,14].

On the one hand, since both chalcopyrite and molybdenite have good floatability, it is generally necessary to add a large amount of chalcopyrite depressant to achieve selective

flotation separation, however, chalcopyrite depressants applied in industry, including sodium cyanide (NaCN), sodium sulfide (Na_2S), and sodium thioglycolate (C_2H_3NaOS), are usually toxic, resulting in environmental hazards and safety problems [15–18]. Currently, several innovative methods have been reported to achieve chalcopyrite depressing and molybdenite flotation by the selective hydrophilic oxidation of the chalcopyrite surface without the addition of depressants, such as thermal pretreatment (250 °C) [19], oxygen plasma pretreatment [20], and electrocatalytic oxidation pretreatment [21]. However, most of them require significant energy costs, so there is a need to develop more cost-effective and environmentally friendly methods.

On the other hand, due to the addition of a large amount of highly dispersible sodium silicate (water glass) in scheelite cleaning flotation, it is necessary to add more precipitants and flocculants to clarify the wastewater [22], which inevitably results in the wastewater containing large numbers of residual flocculants. These residual flocculants, combined with the dissolved metal ions, interfere with or inhibit scheelite flotation, making the wastewater much more difficult to treat and reuse [14]. Although several treatment technologies, such as chemical precipitation, ion exchange, adsorption for metal ions, photocatalytic oxidation and Fenton oxidation for residual organic reagents [5], and membrane separation technologies [23], can be used to convert cleaning flotation wastewater into reusable and qualified water, these methods still have some drawbacks regarding their treatment efficiency and cost.

Compared with molybdenite, the surface oxidation products of chalcopyrite (e.g., CuO, $Cu(OH)_2$, FeOOH, and $Fe_2(SO_4)_3$) are more stable than those of molybdenum (e.g., MoO_3, MoO_4^{2-}, and SO_4^{2-}), especially under acidic or weakly acidic conditions [21,24,25]. Therefore, the natural hydrophobicity of chalcopyrite can be altered, while the surface of molybdenite remains hydrophobic after pretreatment, thus achieving the selective separation of them [21,24,25]. Coincidentally, in the case of Daye Fujiashan Mining Co., Ltd., Huangshi, China, after the addition of sulfuric acid and alum for coagulation precipitation and flocculation pretreatment, the clarified wastewater produced by scheelite cleaning flotation is weakly acidic (pH 4) and contains a lot of metal ions (see detailed description in Section 2.1.2). These factors may provide the feasibility for the surface passivation of chalcopyrite; for example, the presence of H^+, Cu^{2+}, and Fe^{3+} were confirmed to have a positive effect on chalcopyrite oxidation [26].

In this work, the wastewater of the scheelite cleaning flotation process was investigated for the first time for the separation of chalcopyrite and molybdenite using selective surface passivation. Bench-scale flotation experiments were first conducted to separate chalcopyrite and molybdenite samples (including single minerals and artificially mixed minerals) after different periods of immersion pretreatment in the wastewater. Then, the electrochemical cyclic voltammetry of chalcopyrite was studied using chalcopyrite electrodes before and after pretreatment, and the surface properties of the electrodes after pretreatment were also analyzed by SEM and XRD. The mechanism of chalcopyrite passivation in the cleaning flotation wastewater of scheelite is revealed and discussed.

2. Materials and Methods

2.1. Materials

2.1.1. Minerals and Electrodes

The mineral samples with high purity used in this work were collected by hand picking from the Daye Fujiashan Copper-Molybdenum-Tungsten Polymetallic Mine in Hubei Province, China. The compositions of the mineral samples were determined by quantitative X-ray diffraction (Figure 1), and both samples were of high purity (chalcopyrite: 96.65%, molybdenite: 97.02%). Chemical elemental analysis confirmed the elemental compositions of 32.51% Cu, 31.92% Fe, and 33.47% S for the chalcopyrite sample and 55.89% Mo and 35.10% S for the molybdenite sample. A portion of the mineral sample was dry ground to a fine powder by using an agate mortar and then dry sieved to collect a particle size fraction of 38–74+ μm for use as the immersion and flotation mineral samples.

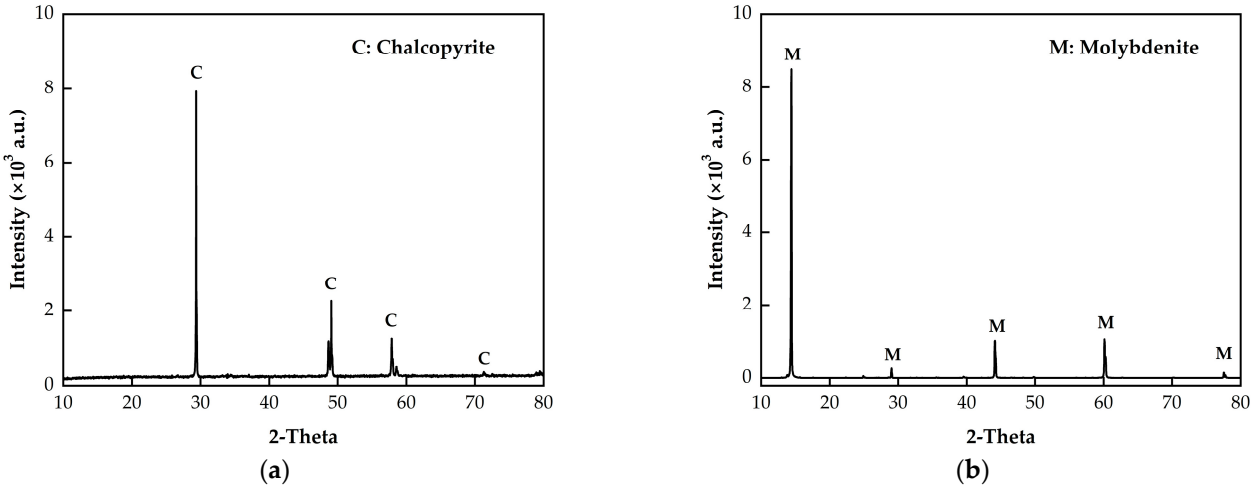

Figure 1. XRD patterns of the samples: (**a**) Chalcopyrite; (**b**) Molybdenite.

A fine crystallized chalcopyrite sample was cut into cylinders (d = 12 mm, h = 5 mm) and selected for the working electrode. The top and bottom surfaces of the cylindrical electrode were polished by using #120, #600, and #1000 silicon carbide papers in that order, and a smoother surface was selected for the electrode working surface. In addition, to reduce oxidation, the mineral samples were sealed in an argon atmosphere prior to use.

2.1.2. Wastewater and Reagents

The wastewater sample was also collected as a slurry from the Daye Fujiashan Copper-Molybdenum-Tungsten Polymetallic Mine in Hubei Province, China. The slurry sample was collected from the scheelite cleaning flotation circuit every 3 h over a 72 h period and mixed. Specifically, the scheelite cleaning flotation circuit consisted of one roughing, seven cleaning, and three scavenging stages, and the wastewater sample was taken from the end of the scavenging stage. The slurry was then supplemented with 5000 mg/L sulfuric acid and 600 mg/L alum, stirred for 1 h and then allowed to stand for 3 h for precipitation. Finally, the supernatant was removed with a pipette and used as the experimental wastewater sample. The chemical composition of the wastewater is shown in Table 1. The wastewater obtained was used in all subsequent experiments. In addition, kerosene (97% purity) and methyl isobutyl carbinol (MIBC) (98% purity) were used as the collector and frother, respectively.

Table 1. Chemical composition of the wastewater (mg/L).

Items	Cu	Pb	Zn	S	Al	Fe	K	Na	Mg	Si	Ca	As	COD [1]	pH
Data	0.15	0.23	0.16	40.71	592	10.32	210	1028	69.12	226	81.0	0.11	85	4.00

[1] COD (Chemical Oxygen Demand) is the oxygen equivalent of substances (usually organic matter) that can be oxidized by strong oxidizing agents in wastewater.

2.2. Methods

2.2.1. Immersion Pretreatment

Immersion pretreatments were performed in 100 mL Erlenmeyer flasks containing 2.0 g of mineral sample or the electrode, 35 mL of wastewater, and shaken at 125 rpm in a shaker (HZL-C, Harbin Donglian Medical Equipment, Harbin, China) at 25 °C for 0 d, 5 d, 10 d, 15 d, and 20 d. Inflatable immersion was also carried out under the same conditions as above, using a microporous air pump (CJY1500, Shanghai Kangyi Instrument, Shanghai, China) to introduce air into the pulp at a flow rate of 50 cm^3/min. The electrode was embedded in an epoxy protector to prevent breakage and erosion of the non-working surface during the immersion process. Water evaporation was compensated for with the

deionized water. The immersion pretreatment and the working electrode assembly are shown in Figure 2.

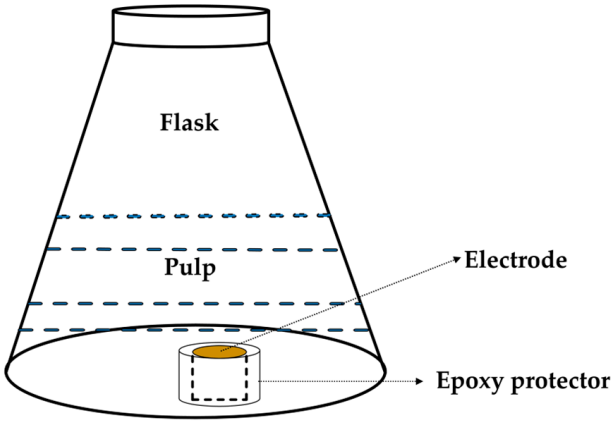

Figure 2. Immersion pretreatment and the working electrode assembly.

2.2.2. Bench-Scale Flotation Experiments

The single mineral and artificially mixed mineral flotation tests were carried out in an XFG flotation machine with a 40 mL plexiglass cell (Wuhan Exploration Machinery Plant, Wuhan, China) at an impeller speed of 1900 rpm at room temperature (25 °C). In each single mineral flotation test, after immersion pretreatment, the pulp was discharged into the cell under continuous agitation (1900 rpm) to form a uniform pulp. Deionized water was used in the flotation experiments. The pH of the pulp was adjusted appropriately by adding NaOH solution (0.1 mol/L) or H_2SO_4 solution (0.1 mol/L), and the mixture was agitated for 4 min. A certain amount of kerosene and MIBC were successively added to the pulp with a conditioning time of 2 min. During the test, after 4 min, the flotation froth began to turn to blank froth and mineral flotation ended; therefore, the flotation time was determined to be 4 min. The concentrates and tailings were then collected, dried, and weighed. Except for when the mass ratio of chalcopyrite to molybdenite was 1:1, the other operations in the artificially mixed mineral flotation tests were the same as those used in the single mineral flotation tests. For the single mineral flotation texts, recovery was calculated based on the weights of dry products recovered. For the artificially mixed mineral flotation tests, recovery was calculated based on the copper and molybdenum grades of the products and the mixed mineral sample (determined by an ARL PERFORM'X XRF spectrometer (Thermo Fisher Scientific, Waltham, MA, USA)).

2.2.3. Electrochemical Experiments

Electrochemical measurements were conducted using a three-electrode system, with chalcopyrite, following immersion pretreatment for different durations, as the working electrode. A saturated calomel electrode (SCE) and a pair of graphite electrodes were used as the reference electrode and counter electrodes, respectively. The electrolyte used was the wastewater from the immersion pretreatment after filtration and clarification. The electrode was removed from the epoxy resin protector without polishing to avoid damaging its surface properties after immersion. In contrast, the surface of the electrode without pretreatment was polished with #1000 silicon carbide paper to ensure that the working surface was fresh prior to the electrochemical experiment. The effective working area of the electrode after encapsulation in the special electrode holder was 0.8 cm^2. Electrochemical measurements were performed using a polarographic analyzer (Model 283, EG&G of Princeton Applied Research, Boston, MA, USA) connected to a computer at a scan rate of 20 mV/s at room temperature (25 °C). In this work, all potentials are reported with respect to the SCE.

2.2.4. SEM and XRD Analysis

X-ray diffraction (XRD, Rigaku, 2500, Tokyo, Japan) and scanning electron microscopy (SEM, Jeoljsm-7500F, Tokyo, Japan) were used to examine the surface composition and morphology of the chalcopyrite after immersion, respectively. The pretreated chalcopyrite and electrodes were filtered and dried using a freeze dryer for SEM and XRD analyses.

3. Results and Discussion

3.1. Flotation of Single Minerals

3.1.1. Effect of Immersion Time

A series of bench-scale flotation tests were conducted to determine the change in the flotation states of single chalcopyrite and molybdenite. Both minerals were immersed in the wastewater for different periods in the presence and absence of aeration. Then, 300 mg/L kerosene as the collector and 100 mg/L MIBC as the frother were used. The pH of the pulp was adjusted to 7 at the start of flotation but was not adjusted during the flotation process. As shown in Figure 3, the recoveries of chalcopyrite and molybdenite without immersion pretreatment (0 d) are 89.12% and 95.61%, respectively, indicating that the floatability of the two minerals is excellent and cannot be successfully separated without the addition of depressants [27], even when kerosene is used as a collector, which has excellent selectivity for molybdenite [28]. With increasing immersion time, regardless of whether the sample was subjected to aeration or not, the recovery of chalcopyrite decreased significantly and the recovery of molybdenite changed only slightly, indicating that immersion in wastewater has a large influence on the floatability of chalcopyrite. The recovery of chalcopyrite without aeration decreased from 89.12% to 60.18% after immersion for 5 days, and even decreased to only 6.28% after immersion for 15 days, indicating that the surface of chalcopyrite might be passivated after immersion. Thus, the longer the immersion time, the more the surface was passivated. It is obvious that the recovery of chalcopyrite after immersion for 10 days with aeration was 5.85%, which is lower than that of 20.17% without aeration. This result shows that the surface passivation of chalcopyrite during immersion can be enhanced by aeration, which could be used to drastically reduce the time required for passivation. Notably, when the immersion time reached 10 days (with aeration) or 15 days (without aeration), the recovery of chalcopyrite had no apparent change with the extension of the immersion time, indicating that the surface passivation of chalcopyrite may be complete at this time. In contrast with chalcopyrite, molybdenite still has excellent floatability after immersion. After 20 days, the recovery of molybdenite with and without aeration was also similar to that of molybdenite without immersion and was still relatively high at 91.28% and 90.23%, respectively. Therefore, it can be assumed that the floatability of molybdenite is slightly affected after immersion.

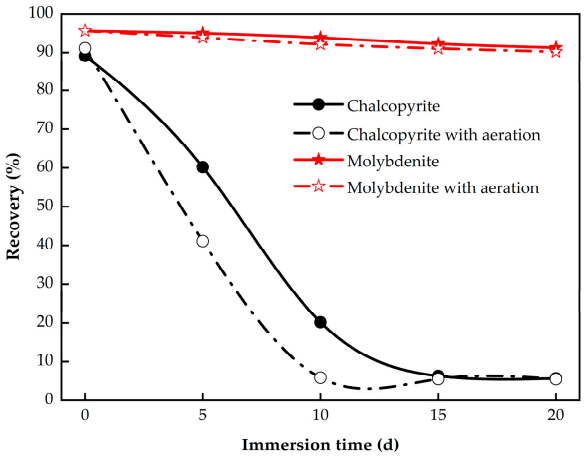

Figure 3. Single mineral flotation recovery of chalcopyrite and molybdenite at different immersion times in the presence and absence of aeration.

The results shown in Figure 3 suggest that the difference in floatability between chalcopyrite and molybdenite can become very significant after immersion in wastewater and can be accelerated by blowing air into the pulp, which provides the possibility and expectation for the selective flotation separation of chalcopyrite and molybdenite by immersion for 10 days with aeration at a flow rate of 50 cm^3/min in wastewater.

3.1.2. Effect of Pulp pH

Minerals typically exhibit different floatabilities at different pulp pH values due to the surface dissolution and modification [16,29]. Therefore, the pulp pH can be used to extend or realize differences in floatability between minerals to achieve selective flotation separation. Figure 4 shows the recoveries of chalcopyrite and molybdenite with and without immersion (10 d and 0 d) pretreatment in the presence of aeration versus pulp pH (the unadjusted initial pH of the pulp was 5). As shown, the recoveries of chalcopyrite and molybdenite without immersion were not affected by the pulp pH and remain around or above 90%. Similarly, in previous reports [16,27,30], both chalcopyrite and molybdenite exhibited stable flotation recoveries (>80%) in the pH range of 3 to 12 using different collectors (sodium dibutyl dithiophosphate, sodium butyl xanthate, and kerosene). However, the recovery of chalcopyrite after immersion was low and did not vary significantly from pH 3 to 11 (between 6.53% and 8.18%). For molybdenite after immersion, the recovery decreased gradually but only slightly with increasing pH, and the recovery could still reach 91.29% at pH 11. Therefore, it can be clearly concluded that pH has no critical effect on the floatability of chalcopyrite and molybdenite with and without immersion.

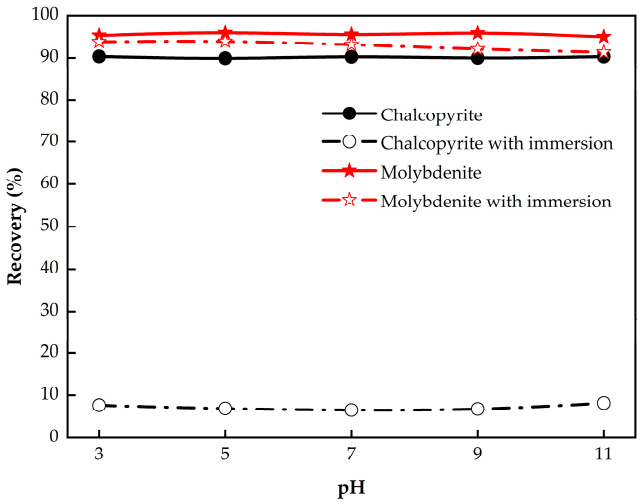

Figure 4. Single mineral flotation recoveries of chalcopyrite and molybdenite with different pulp pH with and without immersion.

3.1.3. Effect of Collector Dosage

The effect of the dosage of kerosene as a collector on the flotation behavior of chalcopyrite and molybdenite was tested under the condition that the dosage of MIBC was fixed at 100 mg/L. As the pulp pH was proven to have no critical effect on the floatability of chalcopyrite and molybdenite, the pulp pH was still adjusted to 7 prior to flotation, and no further adjustments were made during the flotation process. The results are shown in Figure 5. In the absence of kerosene, the recoveries of chalcopyrite and molybdenite without immersion pretreatment were 57.05% and 65.29%, respectively, demonstrating that both minerals have excellent natural floatability and that the floatability of molybdenite is slightly better than that of chalcopyrite [27,31,32]. In contrast, the recovery of chalcopyrite after 10 days of immersion with aeration decreased sharply to only 6.12% in the absence of kerosene. However, the recovery of molybdenite after immersion was still up to 62.58%. It can be concluded that immersion pretreatment can significantly enhance the hydrophilicity

of chalcopyrite, thereby reducing its floatability. The recovery of chalcopyrite without immersion is related to kerosene dosage, which increases with increasing kerosene dosage and reaches an equilibrium peak when the amount of kerosene exceeds 300 mg/L. However, the recovery of chalcopyrite after immersion did not change with increasing kerosene dosage and remained at the very low level of approximately 7%. This might be attributed to the passivation layer formed on the surface of the chalcopyrite after immersion, which prevents the adsorption of kerosene. Regardless of whether it was pretreated with immersion or not, the correlations between molybdenite recovery and kerosene dosage were similar, and both increased with increasing kerosene dosage until reaching the equilibrium peak, further indicating that the floatability of molybdenite is not only excellent but also extremely stable. As mentioned above [21,24,25], the surface of chalcopyrite is more easily oxidized, and the oxidation products of chalcopyrite are more stable than those of molybdenum. Therefore, the flotation inhibition effect of chalcopyrite can be related to the accumulation of oxidation products on the surface of chalcopyrite after immersion. Meanwhile, there should be no oxidation product accumulation on the surface of molybdenum, so its floatability is not affected by pretreatment.

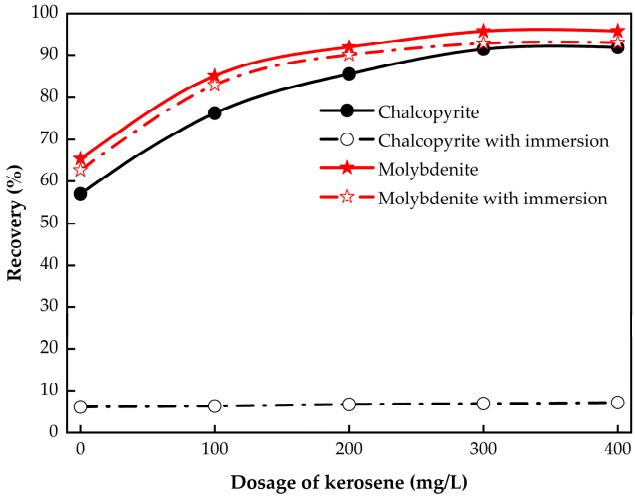

Figure 5. Single mineral flotation recovery of chalcopyrite and molybdenite with various kerosene dosages with and without immersion.

3.2. Flotation of Artificially Mixed Minerals

Following the results of single mineral flotation, the selective flotation separation of artificially mixed minerals was carried out to verify the effect of immersion pretreatment in the wastewater of the scheelite cleaning flotation process. The mass ratio of chalcopyrite to molybdenite used in each test was 1:1 in the mixed minerals. The dosages of kerosene and MIBC were 350 mg/L and 100 mg/L, respectively, and the pulp pH was adjusted to 7 prior to flotation during the tests. The results are shown in Figure 6. Without immersion pretreatment, chalcopyrite and molybdenite were almost completely enriched in the froth concentrate, with recoveries of 93.04% and 95.50%, respectively, indicating that the selective separation of chalcopyrite and molybdenite by flotation cannot be achieved without pretreatment. After 15 days of immersion (without aeration), the recoveries of chalcopyrite and molybdenite in the froth concentrate were 9.03% and 94.13%, respectively. In addition, a lower recovery of chalcopyrite (6.91%) could be achieved while the recovery of molybdenite remained constant (93.03%) after 15 days of immersion (with aeration), which is also consistent with the results obtained for single minerals. The slight difference between the two tests is that the recovery of chalcopyrite in the artificial mixed mineral test was 2% to 5% greater than that in the single mineral test, regardless of immersion or aeration, which may be due to the mechanical entrainment in the mixed mineral flotation process [33–35]. In summary, these results indicate that the effective flotation separation

of chalcopyrite and molybdenite can be achieved by immersion pretreatment using the wastewater from scheelite cleaning flotation. Compared with traditional methods, the immersion pretreatment method avoids the use of massive amounts of environmentally harmful depressants while alleviating the problem of wastewater reuse. However, this method still has some drawbacks, such as a relatively long immersion process and the need for special requirements (such as corrosion resistance). Further research is needed to reduce the immersion time and optimize the equipment investment.

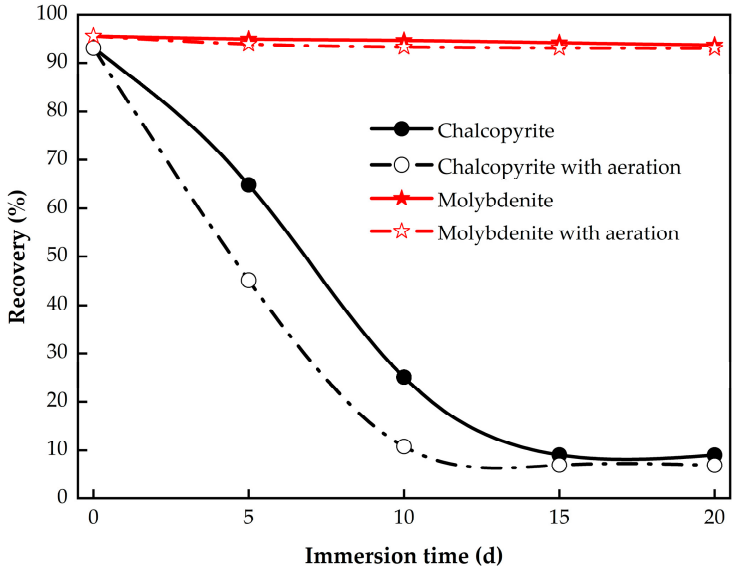

Figure 6. Mixed mineral flotation recovery of chalcopyrite and molybdenite with different immersion times in the presence and absence of aeration.

3.3. Electrochemical Mechanism

In order to investigate the mechanism of chalcopyrite passivation during the immersion process, cyclic voltammetry was used to detect the variation in electrochemical behavior on the chalcopyrite surface in the wastewater from scheelite cleaning flotation. All tests were scanned from −600 mV to 800 mV and then back to −600 mV. The cyclic voltammetry curves of the electrodes after different durations of immersion without and with aeration are shown in Figure 7.

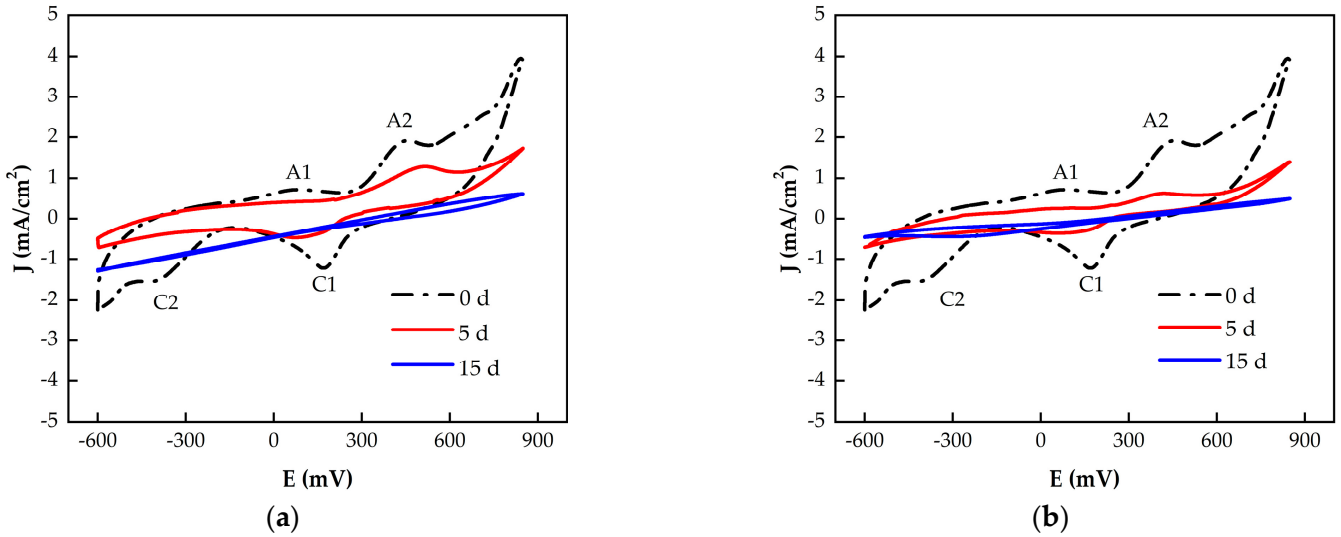

Figure 7. Cyclic voltammetry curves of the electrodes with different immersion times: (**a**) without aeration; (**b**) with aeration.

As shown in Figure 7a, the electrochemical behavior of the electrode at different immersion times without aeration was significantly different. The oxidation peaks A1 and A2 and the reduction peaks C1 and C2 on the cyclic voltammetry curves were significant without immersion (0 d). In the anodic scan, the voltammograms show a pre-peak A1, which could be attributed to the formation of a non-stoichiometric polysulfide phase ($Cu_{1-x}Fe_{1-y}S_{2-z}$), since the chalcopyrite surface favors the release of iron, as shown in Equation (1) [36–39]. The non-stoichiometric polysulfide phase is an intermediate product that mixes with S^0 and forms a passive electron conducting layer on the chalcopyrite surface. At peak A2, the layers of $Cu_{1-x}Fe_{1-y}S_{2-z}$ and chalcopyrite could both be destroyed and oxidized, as shown in Equations (2) and (3) [36–40].

$$CuFeS_2 \rightarrow Cu_{1-x}Fe_{1-y}S_{2-z} + xCu^{2+} + yFe^{2+} + zS^0 + 2(x+y)e^- \ (y >> x), \quad (1)$$

$$Cu_{1-x}Fe_{1-y}S_{2-z} \rightarrow (1-x)Cu^{2+} + (1-y)Fe^{2+} + (2-z)S + 2(2-x-y)e^-, \quad (2)$$

$$CuFeS_2 \rightarrow Cu^{2+} + Fe^{3+} + 2S + 5e^-, \quad (3)$$

In the cathodic reverse scan, there are two reduction peaks, C1 and C2. Peak C1 should correspond to the reduction in the products produced at peaks A1 and A2. The reduction reactions mainly involve the participation of copper ions, as shown in Equations (4)–(9). Peak C2 reflects the reduction of the remaining chalcopyrite to an intermediate copper sulfide such as $Cu_9Fe_8S_{16}$ or Cu_5FeS_4, as shown in Equations (10) and (11) [36–39].

$$Cu^{2+} + S^0 + 2e^- \rightarrow CuS, \quad (4)$$

$$Cu^{2+} + CuS + 2e^- \rightarrow Cu_2S, \quad (5)$$

$$Cu^{2+} + 2e^- \rightarrow Cu^0, \quad (6)$$

$$3Cu^{2+} + CuFeS_2 + 4e^- \rightarrow 2Cu_2S + Fe^{2+}, \quad (7)$$

$$3Cu^{2+} + 2CuFeS_2 + 4e^- \rightarrow Cu_5FeS_4 + Fe^{2+}, \quad (8)$$

$$2CuS + 2H^+ + 2e^- \rightarrow Cu_2S + H_2S, \quad (9)$$

$$9CuFeS_2 + 4H^+ + 2e^- \rightarrow Cu_9Fe_8S_{16} + Fe^{2+} + 2H_2S, \quad (10)$$

$$5CuFeS_2 + 12H^+ + 4e^- \rightarrow Cu_5FeS_4 + 4Fe^{2+} + 6H_2S, \quad (11)$$

After 5 days of immersion, the oxidation and reduction peaks all became weak. Peak A1 almost disappeared, indicating that peak A1 was inhibited first. After 15 days, peaks A1 and C1 completely disappeared, and peak A2 became extremely weak. Similar to the bioleaching system of chalcopyrite, the electrode surface after pretreatment could be covered with a passive film that is non-conductive or difficult to conduct electricity, and any reactions that occurred on the surface would be suppressed at this time [41]. In detail, passivation species such as iron-hydroxy precipitates, jarosite, and non-stoichiometric polysulfide phases could be formed during the immersion process, as shown in Equations (1) and (12)–(15) (Note: K^+ in Equations (14) and (15) can be replaced by Na^+, NH_4^+, and H_3O^+.) [38,42,43].

$$2Fe^{2+} + 2H^+ + 0.5O_2 \rightarrow 2Fe^{3+} + H_2O, \quad (12)$$

$$2Fe^{3+} + 4H_2O \rightarrow 2FeOOH + 6H^+, \quad (13)$$

$$2Fe^{3+} + K^+ + 2SO_4^{2-} + FeOOH + 4H_2O \rightarrow KFe_3(SO_4)_2(OH)_6 + 3H^+, \quad (14)$$

$$3Fe^{3+} + 2SO_4^{2-} + 6H_2O + K^+ \rightarrow KFe_3(SO_4)_2(OH)_6 + 6H^+, \quad (15)$$

Furthermore, the cyclic voltammetry curves for the electrodes at different immersion times with aeration are shown in Figure 7b, which are basically consistent with no aeration, but the changes are more obvious and rapid. After 5 days, all the peaks almost disappeared, indicating that the electrode surface was significantly passivated. As shown in

Equations (1) and (12)–(15), oxygen can accelerate the oxidation of Fe^{2+} and the formation of FeOOH and jarosite during the immersion process so that the aeration can obviously promote the passivation of the chalcopyrite surface and shorten the passivation time.

3.4. Changes in Chalcopyrite Surface Morphology and Composition

The SEM image (magnified 2000 times) of chalcopyrite after 15 days of immersion is shown in Figure 8. As shown, a large number of particles with approximate spherical shape, mostly aggregates, were generated on the surface of chalcopyrite, which is similar to the morphology of jarosite reported in the other literature [44]. Similar to other depressant-free flotation separation methods [19–21] for copper-molybdenum ore, the immersion pretreatment significantly modified the surface of chalcopyrite. In detail, insoluble oxidation products including CuO, $Cu(OH)_2$, and FeOOH (especially FeOOH) were detected on the chalcopyrite surface after thermal pretreatment [19], oxygen plasma pretreatment [20], or electrocatalytic oxidation pretreatment [21].

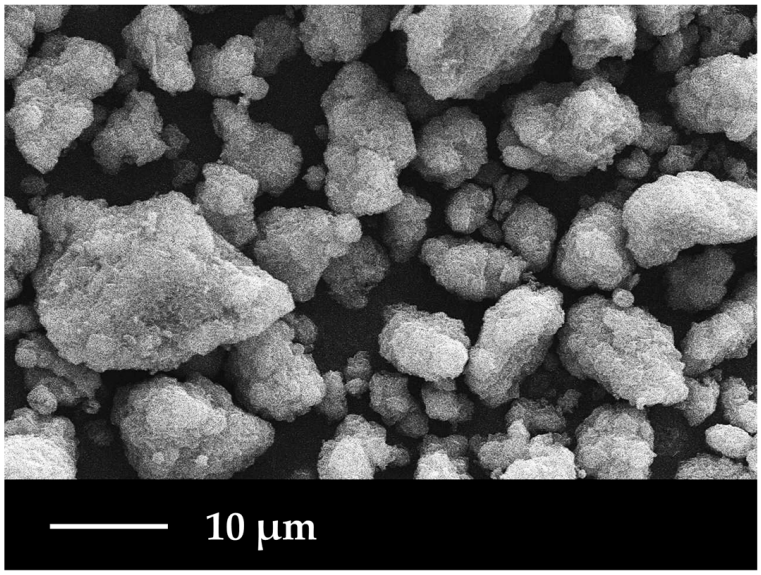

Figure 8. SEM image of the chalcopyrite sample after 15 days of immersion.

For further clarification of the composition of the surface products, X-ray diffraction of chalcopyrite after 15 days of immersion was performed. As shown in Figure 9, obvious peaks belonging to jarosite were detected. Although no FeOOH peaks were observed, it may appear as an intermediate of jarosite on the chalcopyrite surface during the immersion pretreatment process [38,42,43]. According to the reports of [19–21], soluble $Fe_2(SO_4)_3$ and MoO_3/MoO_4^{2-} were also the obvious oxidation products of chalcopyrite and molybdenum during the pretreatment process, respectively. Therefore, the presence of Fe^{3+} could promote the transformation from FeOOH to jarosite, as shown in Equation (14).

According to the results of XRD and SEM, after immersion pretreatment, the surface of chalcopyrite was heavily covered with oxidation products mainly composed of jarosite, which was consistent with the passivation phenomenon in electrochemical experiments. Importantly, the FeOOH and jarosite formed are highly hydrophilic [45–47], and the water contact angles of chalcopyrite before and after oxidation pretreatment were reported to decrease from ~80° to ~40° and ~20° [20,21]. However, the surface oxidation products of molybdenum were dissolved during the pretreatment process [19–21,24,25], leaving a fresh surface with a great floatability (water contact angles ~85°). Therefore, the different surface transformations of chalcopyrite and molybdenum during the immersion pretreatment process should be responsible for their successful separation.

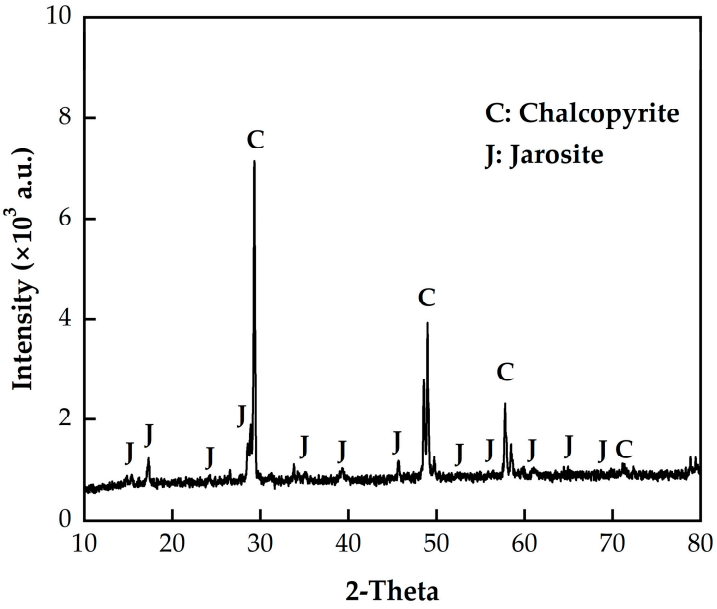

Figure 9. XRD pattern of the chalcopyrite sample after 15 days of immersion.

4. Conclusions

The use of flotation wastewater from scheelite cleaning flotation for the separation of chalcopyrite and molybdenite by selective surface passivation was investigated for the first time in this work. The flotation of chalcopyrite can be effectively suppressed after immersion pretreatment using the wastewater from scheelite cleaning flotation, while the flotation of molybdenite was only slightly affected. Pulp pH was proven to have no effect on the flotation of either mineral, while the addition of aeration during the immersion process can apparently shorten the passivation time by forming passivation species (especially jarosite) on the surface of chalcopyrite. The effective copper-molybdenum separation (molybdenite 93.22%, chalcopyrite 10.77%) can be achieved under the conditions of immersion pretreatment for 10 days with aeration at an air flow rate of 50 cm^3/min in the wastewater, 350 mg/L of kerosene collector, 100 mg/L of MIBC frother, and an initial pH of 7. The results obtained achieved the flotation separation of molybdenite and chalcopyrite without the use of depressants, while using wastewater to selectively oxidize chalcopyrite avoids the high costs of other chemical or electrochemical oxidation methods, thus demonstrating wide application prospects.

Author Contributions: Conceptualization, G.G. and Y.G.; methodology, G.G.; validation, Y.G.; investigation, Y.G.; resources, G.G. and Y.W.; data curation, Y.G.; writing—original draft preparation, Y.G.; writing—review and editing, G.G., Y.G., Y.Z., Q.L., S.L. and Y.W.; visualization, Y.G.; supervision, G.G.; project administration, G.G. and Y.W.; funding acquisition, G.G. and Y.W. All authors have read and agreed to the published version of the manuscript.

Funding: This research was funded by National Natural Science Foundation of China, grant numbers 52104288 and 52074358.

Data Availability Statement: The data presented in this study are available on request from the corresponding author. The data are not publicly available due to the terms of the project.

Acknowledgments: The authors would like to thank Shiyanjia Lab (www.shiyanjia.com, accessed on 23 September 2023) for their support in the XRD test.

Conflicts of Interest: The authors declare no conflicts of interest.

References

1. Sun, Z.; Wang, Q. The asymmetric effect of natural resource abundance on economic growth and environmental pollution: Evidence from resource-rich economy. *Resour. Policy* **2021**, *72*, 102085. [CrossRef]
2. Jing, G.; Meng, X.; Sun, W.; Kowalczuk, P.B.; Gao, Z. Recent advances in the treatment and recycling of mineral processing wastewater. *Environ. Sci. Water Res. Technol.* **2023**, *9*, 1290–1304. [CrossRef]
3. Lin, S.; Liu, R.; Wu, M.; Hu, Y.; Sun, W.; Shi, Z.; Han, H.; Li, W. Minimizing beneficiation wastewater through internal reuse of process water in flotation circuit. *J. Clean. Prod.* **2020**, *245*, 118898. [CrossRef]
4. Azevedo, A.; Oliveira, H.; Rubio, J. Treatment and water reuse of lead-zinc sulphide ore mill wastewaters by high rate dissolved air flotation. *Miner. Eng.* **2018**, *127*, 114–121. [CrossRef]
5. Meng, S.; Wen, S.; Han, G.; Wang, X.; Feng, Q. Wastewater Treatment in Mineral Processing of Non-Ferrous Metal Resources: A Review. *Water* **2022**, *14*, 726. [CrossRef]
6. Wan, H.; Qu, J.; He, T.; Bu, X.; Yang, W.; Li, H. A New Concept on High-Calcium Flotation Wastewater Reuse. *Minerals* **2018**, *8*, 496. [CrossRef]
7. Jing, G.; Ren, S.; Gao, Y.; Sun, W.; Gao, Z. Electrocoagulation: A Promising Method to Treat and Reuse Mineral Processing Wastewater with High COD. *Water* **2020**, *12*, 595. [CrossRef]
8. Jing, G.; Wang, J.; Sun, W.; Pooley, S.; Liao, D.; Shi, Z.; Chen, Q.; Gao, Z. Reuse of mine and ore washing wastewater in scheelite flotation process to save freshwater: Lab to industrial scale. *J. Water Process Eng.* **2023**, *53*, 103674. [CrossRef]
9. Yang, X. Beneficiation studies of tungsten ores—A review. *Miner. Eng.* **2018**, *125*, 111–119. [CrossRef]
10. Jin, W.; Yang, S.; Tang, C.; Li, Y.; Chang, C.; Chen, Y. Reaction Mechanism and Technical Application of Metallic Bismuth Extraction from Bismuthinite Concentrate by Low-Temperature Alkaline Smelting. *ACS Sustain. Chem. Eng.* **2023**, *11*, 9932–9946. [CrossRef]
11. Li, W.-C.; Yu, H.-J.; Gao, X.; Liu, X.-L.; Wang, J.-H. Review of Mesozoic multiple magmatism and porphyry Cu–Mo (W) mineralization in the Yidun Arc, eastern Tibet Plateau. *Ore Geol. Rev.* **2017**, *90*, 795–812. [CrossRef]
12. Yang, B.; Zeng, M.; Zhu, H.; Huang, P.; Li, Z.; Song, S. Selective depression of molybdenite using a novel eco-friendly depressant in Cu-Mo sulfides flotation system. *Colloids Surf. A Physicochem. Eng. Asp.* **2021**, *622*, 126683. [CrossRef]
13. Wang, X.; Qin, W.-Q.; Jiao, F.; Yang, C.-R.; Li, W.; Zhang, Z.-Q.; Zhou, J.-M.; Guo, J.-G.; Zhang, J. Review on development of low-grade scheelite recovery from molybdenum tailings in Luanchuan, China: A case study of Luoyang Yulu Mining Company. *Trans. Nonferr. Met. Soc. China* **2022**, *32*, 980–998. [CrossRef]
14. Kang, J.; Chen, C.; Sun, W.; Tang, H.; Yin, Z.; Liu, R.; Hu, Y.; Nguyen, A.V. A significant improvement of scheelite recovery using recycled flotation wastewater treated by hydrometallurgical waste acid. *J. Clean. Prod.* **2017**, *151*, 419–426. [CrossRef]
15. Yan, H.; Yang, B.; Zeng, M.; Huang, P.; Teng, A. Selective flotation of Cu-Mo sulfides using xanthan gum as a novel depressant. *Miner. Eng.* **2020**, *156*, 106486. [CrossRef]
16. Yi, G.; Macha, E.; Van Dyke, J.; Macha, R.E.; McKay, T.; Free, M.L. Recent progress on research of molybdenite flotation: A review. *Adv. Colloid Interface Sci.* **2021**, *295*, 102466. [CrossRef] [PubMed]
17. Hao, J.; Liu, J.; Yu, Y.; Gao, H.; Qin, X.; Bai, X. Depressants for separation of chalcopyrite and molybdenite: Review and prospects. *Miner. Eng.* **2023**, *201*, 108209. [CrossRef]
18. Peng, H.; Wu, D.; Abdalla, M.; Luo, W.; Jiao, W.; Bie, X. Study of the Effect of Sodium Sulfide as a Selective Depressor in the Separation of Chalcopyrite and Molybdenite. *Minerals* **2017**, *7*, 51. [CrossRef]
19. Tang, X.; Chen, Y.; Liu, K.; Zeng, G.; Peng, Q.; Li, Z. Selective flotation separation of molybdenite and chalcopyrite by thermal pretreatment under air atmosphere. *Colloids Surf. A Physicochem. Eng. Asp.* **2019**, *583*, 123958. [CrossRef]
20. Hirajima, T.; Mori, M.; Ichikawa, O.; Sasaki, K.; Miki, H.; Farahat, M.; Sawada, M. Selective flotation of chalcopyrite and molybdenite with plasma pre-treatment. *Miner. Eng.* **2014**, *66–68*, 102–111. [CrossRef]
21. Peng, W.; Liu, S.; Cao, Y.; Wang, W.; Lv, S.; Huang, Y. A novel approach for selective flotation separation of chalcopyrite and molybdenite—Electrocatalytic oxidation pretreatment and its mechanism. *Appl. Surf. Sci.* **2022**, *597*, 153753. [CrossRef]
22. Kang, J.; Fan, R.; Hu, Y.; Sun, W.; Liu, R.; Zhang, Q.; Liu, H.; Meng, X. Silicate removal from recycled wastewater for the improvement of scheelite flotation performance. *J. Clean. Prod.* **2018**, *195*, 280–288. [CrossRef]
23. Awadalla, F.T.; Kumar, A. Opportunities for Membrane Technologies in the Treatment of Mining and Mineral Process Streams and Effluents. *Sep. Sci. Technol.* **1994**, *29*, 1231–1249. [CrossRef]
24. Hirajima, T.; Miki, H.; Suyantara, G.P.W.; Matsuoka, H.; Elmahdy, A.M.; Sasaki, K.; Imaizumi, Y.; Kuroiwa, S. Selective flotation of chalcopyrite and molybdenite with H_2O_2 oxidation. *Miner. Eng.* **2017**, *100*, 83–92. [CrossRef]
25. Miki, H.; Matsuoka, H.; Hirajima, T.; Suyantara, G.P.W.; Sasaki, K. Electrolysis Oxidation of Chalcopyrite and Molybdenite for Selective Flotation. *Mater. Trans.* **2017**, *58*, 761–767. [CrossRef]
26. Li, Y.; Kawashima, N.; Li, J.; Chandra, A.P.; Gerson, A.R. A review of the structure, and fundamental mechanisms and kinetics of the leaching of chalcopyrite. *Adv. Colloid Interface Sci.* **2013**, *197*, 1–32. [CrossRef]
27. Yin, Z.; Chen, S.; Xu, Z.; Zhang, C.; He, J.; Zou, J.; Chen, D.; Sun, W. Flotation separation of molybdenite from chalcopyrite using an environmentally-efficient depressant L-cysteine and its adsoption mechanism. *Miner. Eng.* **2020**, *156*, 106438. [CrossRef]
28. Li, H.; Xiao, W.; Jin, J.; Han, Y. Influence Mechanism of Magnetized Modified Kerosene on Flotation Behavior of Molybdenite. *Minerals* **2022**, *12*, 2. [CrossRef]
29. Irannajad, M.; Nuri, O.S.; Mehdilo, A. Surface dissolution-assisted mineral flotation: A review. *J. Environ. Chem. Eng.* **2019**, *7*, 103050. [CrossRef]

30. Wang, Z.; Qian, Y.; Xu, L.-H.; Dai, B.; Xiao, J.-H.; Fu, K. Selective chalcopyrite flotation from pyrite with glycerine-xanthate as depressant. *Miner. Eng.* **2015**, *74*, 86–90. [CrossRef]
31. Wang, X.; Zhao, B.; Liu, J.; Zhu, Y.; Han, Y. Dithiouracil, a highly efficient depressant for the selective separation of molybdenite from chalcopyrite by flotation: Applications and mechanism. *Miner. Eng.* **2022**, *175*, 107287. [CrossRef]
32. Zhang, X.; Lu, L.; Cao, Y.; Yang, J.; Che, W.; Liu, J. The flotation separation of molybdenite from chalcopyrite using a polymer depressant and insights to its adsorption mechanism. *Chem. Eng. J.* **2020**, *395*, 125137. [CrossRef]
33. Yang, J.; Chen, L.; Xue, Z.; Yang, K.; Shao, Y.; Zeng, J.; Gao, Y. Performance evaluation of PHGMS technology for superfine chalcopyrite-molybdenite separation. *Sep. Purif. Technol.* **2024**, *336*, 126136. [CrossRef]
34. Park, I.; Hong, S.; Jeon, S.; Ito, M.; Hiroyoshi, N. Flotation Separation of Chalcopyrite and Molybdenite Assisted by Microencapsulation Using Ferrous and Phosphate Ions: Part I. *Selective Coating Formation. Metals* **2020**, *10*, 1667. [CrossRef]
35. Abdollahi, M.; Bahrami, A.; Mirmohammadi, M.S.; Kazemi, F.; Danesh, A.; Ghorbani, Y. A process mineralogy approach to optimize molybdenite flotation in copper–molybdenum processing plants. *Miner. Eng.* **2020**, *157*, 106557. [CrossRef]
36. Zhao, H.; Zhang, Y.; Zhang, X.; Qian, L.; Sun, M.; Yang, Y.; Zhang, Y.; Wang, J.; Kim, H.; Qiu, G. The dissolution and passivation mechanism of chalcopyrite in bioleaching: An overview. *Miner. Eng.* **2019**, *136*, 140–154. [CrossRef]
37. Ghahremaninezhad, A.; Asselin, E.; Dixon, D. Electrochemical evaluation of the surface of chalcopyrite during dissolution in sulfuric acid solution. *Electrochim. Acta* **2010**, *55*, 5041–5056. [CrossRef]
38. Zhang, Y.; Zhao, H.; Qian, L.; Sun, M.; Lv, X.; Zhang, L.; Petersen, J.; Qiu, G. A brief overview on the dissolution mechanisms of sulfide minerals in acidic sulfate environments at low temperatures: Emphasis on electrochemical cyclic voltammetry analysis. *Miner. Eng.* **2020**, *158*, 106586. [CrossRef]
39. Gu, G.; Hu, K.; Zhang, X.; Xiong, X.; Yang, H. The stepwise dissolution of chalcopyrite bioleached by *Leptospirillum ferriphilum*. *Electrochim. Acta* **2013**, *103*, 50–57. [CrossRef]
40. Córdoba, E.; Muñoz, J.; Blázquez, M.; González, F.; Ballester, A. Leaching of chalcopyrite with ferric ion. Part I: General aspects. *Hydrometallurgy* **2008**, *93*, 81–87. [CrossRef]
41. Lv, X.; Wang, J.; Zeng, X.; Liang, Z.; He, D.; Zhang, Y.; Yuan, H.; Zhao, H.; Meng, Q. Cooperative extraction of metals from chalcopyrite by bio-oxidation and chemical oxidation. *Geochemistry* **2021**, *81*, 125772. [CrossRef]
42. Ahmadi, A.; Schaffie, M.; Manafi, Z.; Ranjbar, M. Electrochemical bioleaching of high grade chalcopyrite flotation concentrates in a stirred bioreactor. *Hydrometallurgy* **2010**, *104*, 99–105. [CrossRef]
43. Córdoba, E.; Muñoz, J.; Blázquez, M.; González, F.; Ballester, A. Leaching of chalcopyrite with ferric ion. Part II: Effect of redox potential. *Hydrometallurgy* **2008**, *93*, 88–96. [CrossRef]
44. Gunneriusson, L.; Sandström, A.; Holmgren, A.; Kuzmann, E.; Kovacs, K.; Vértes, A. Jarosite inclusion of fluoride and its potential significance to bioleaching of sulphide minerals. *Hydrometallurgy* **2009**, *96*, 108–116. [CrossRef]
45. Yan, B.; Liang, T.; Yang, X.; Gadgil, A.J. Superior removal of As(III) and As(V) from water with Mn-doped β-FeOOH nanospindles on carbon foam. *J. Hazard. Mater.* **2021**, *418*, 126347. [CrossRef] [PubMed]
46. Chen, Q.; Yao, Y.; Zhao, Z.; Zhou, J.; Chen, Z. Long term catalytic activity of pyrite in Heterogeneous Fenton-like oxidation for the tertiary treatment of dyeing wastewater. *J. Environ. Chem. Eng.* **2021**, *9*, 105730. [CrossRef]
47. Karthe, S.; Szargan, R.; Suoninen, E. Oxidation of pyrite surfaces: A photoelectron spectroscopic study. *Appl. Surf. Sci.* **1993**, *72*, 157–170. [CrossRef]